



UNIVERSITY OF GOTHENBURG

This is a copy of an article published in Journal of Applied Physics © 2015 AIP Publishing LLC; Journal of Applied Physics is available online at:
<http://scitation.aip.org/content/aip/journal/jap>.

Citation for the published paper:

Thickness- and temperature-dependent magnetodynamic properties of yttrium iron garnet thin films

M. Haidar, M. Ranjbar, M. Balinsky, R. K. Dumas, S. Khartsev and J. Åkerman
J. Appl. Phys. 117, 17D119 (2015); <http://dx.doi.org/10.1063/1.4914363>

GUP

Gothenburg University Publications

<http://gup.ub.gu.se>

Thickness- and temperature-dependent magnetodynamic properties of yttrium iron garnet thin films

M. Haidar,^{1,a)} M. Ranjbar,¹ M. Balinsky,¹ R. K. Dumas,¹ S. Khartsev,² and J. Åkerman^{1,3}

¹Department of Physics, University of Gothenburg, 41296 Gothenburg, Sweden

²Department of Integrated Devices and Circuits, School of ICT, Royal Institute of Technology (KTH), 16440 Kista, Sweden

³Materials Physics, School of ICT, Royal Institute of Technology (KTH), 16440 Kista, Sweden

(Presented 7 November 2014; received 21 September 2014; accepted 2 November 2014; published online 10 March 2015)

The magnetodynamical properties of nanometer-thick yttrium iron garnet films are studied using ferromagnetic resonance as a function of temperature. The films were grown on gadolinium gallium garnet substrates by pulsed laser deposition. First, we found that the damping coefficient increases as the temperature increases for different film thicknesses. Second, we found two different dependencies of the damping on film thickness: at room temperature, the damping coefficient increases as the film thickness decreases, while at $T=8$ K, we find the damping to depend only weakly on the thickness. We attribute this behavior to an enhancement of the relaxation of the magnetization by impurities or defects at the surfaces. © 2015 AIP Publishing LLC. [<http://dx.doi.org/10.1063/1.4914363>]

The utilization of spin waves (SWs) is critical to the fields of magnonics and spintronics, due to the tremendous potential of spin waves in data storage and signal processing.^{1,2} However, the common ferromagnetic materials used in spintronic devices are not ideal for SW propagation due to their high Gilbert damping. The solution lies in using materials with ultralow damping, such as yttrium iron garnet (YIG).^{3,4} The intrinsic damping of bulk YIG is $\alpha = 10^{-5}$,⁵ which is two orders of magnitude smaller than that of ferromagnetic metals, such as permalloy. However, recent studies have shown that YIG films are also suitable for spintronics applications because (i) they are electrical insulators and (ii) they generate a pure spin current at the interfaces with a normal metal via spin pumping and the spin Seebeck effect.^{6–14} The emergence of YIG-based devices in spintronics applications requires (i) the fabrication of nanometer-thick YIG films and (ii) a fundamental investigation of the magnetodynamics properties of YIG on the nanoscale. The quality of such thin YIG films depends strongly on the growth process. Considerable efforts have been made towards growing high-quality thin YIG films using pulsed laser deposition (PLD)^{15–18} and sputtering¹⁹ techniques, in which the properties of the films converge to the bulk properties. Magnetodynamical studies using ferromagnetic resonance (FMR) have been primarily performed only at room temperature. Additionally, transport measurements have demonstrated a new type of magnetoresistance, known as spin Hall magnetoresistance (SMR), which has been detected at room temperature and low temperature.^{20–22} Despite the rapid progress in YIG thin-film fabrication and room temperature characterization, the temperature dependence of the magnetodynamic properties is still lacking.

In this proceeding, we report on the temperature dependence of the magnetodynamic properties of YIG thin films. We perform FMR measurements at variable temperatures (8–300 K). We observe an increase in the Gilbert damping value as the temperature increases. This behavior is observed over a wide range of film thicknesses of 30–170 nm. We find that the damping coefficient increases as the film thickness decreases at room temperature. However, the damping is found to be independent of film thickness for low temperatures. Additionally, for our thinnest films (=20 nm), we find a nonlinear increase in the linewidth as a function of the frequency, which indicates the presence of the two-magnon scattering process.

YIG films were grown on (111) oriented single crystal ($\text{Gd}_3\text{Ga}_5\text{O}_{12}$, GGG) substrates by PLD techniques. 1.5-in. high density stoichiometric $\text{Y}_3\text{Fe}_5\text{O}_{12}$ target was ablated using 248 nm CompexPro 110 excimer laser at energy density of 3.4 J/cm^2 and 30 Hz repetition rate. Films were grown in the vacuum system (ultimate pressure 10^{-8}) at substrate temperature of 760°C , target to substrate distance of 100 mm and having oxygen as background gas at pressure of 25 mTorr. Films were *in situ* postannealed at deposition temperature and oxygen pressure of 300 Torr. As our primary focus is to study the dynamics of thin YIG films, we fabricated and measured films with the following thicknesses: 170, 65, 40, 30, and 20 nm.

The surface roughness of the films was measured using atomic force microscopy (AFM). The AFM analysis revealed a smooth and uniform surface with a root mean squared roughness of $0.3 \pm 0.02 \text{ nm}$, as shown in Fig. 1(a). For variable temperature FMR measurements we used a NanoOsc Instruments CryoFMR in a Montana Instruments Cryostation. The sample was placed on a coplanar waveguide (CPW) in a flip-chip configuration, and the variation of the absorbed power (dP/dH) was measured as the

^{a)}Electronic mail: mohammad.haidar@Physics.gu.se.

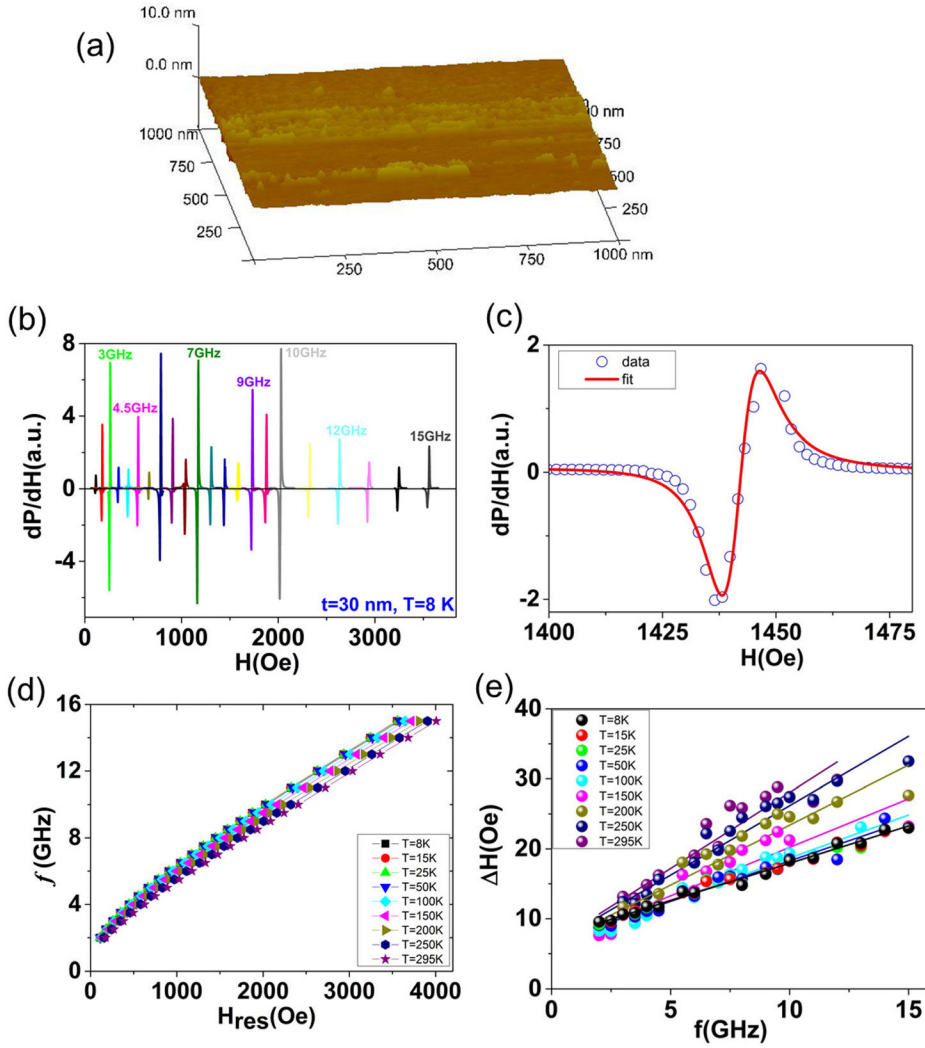


FIG. 1. Properties of a 30 nm thick YIG film: (a) AFM surface image; (b) and (c) FMR spectra measured at $T = 8$ K for different frequencies; the solid red line in (c) is a fit; (d) the variation of the frequency with respect to the field at different temperatures; and (e) the variation of the linewidth as a function of the frequency at different temperatures. In all graphs, the points show the experimental data and the curves show the fits.

magnetic field was swept at different temperatures. The magnetic field was applied in the film plane and the measurements were carried out at various temperatures between 8 and 295 K. At each temperature, the FMR response was measured at several frequencies over the range of 2–16 GHz. At each frequency, the resonance field (H_{res}) and the linewidth (ΔH) of the FMR signal were determined. Fig. 1(b) shows the FMR spectra measured for the 30 nm film at different frequencies at 8 K. Fig. 1(c) gives the FMR profile measured at $f = 8$ GHz at 8 K. Fig. 1(d) shows the variation of the frequency as a function of the resonance field, while Fig. 1(e) shows the variation of the linewidth as a function of the frequency at different temperatures. In Fig. 1(c), the solid line shows the fit to a derivative of a symmetric and antisymmetric Lorentzian function from which the resonance field and the linewidth were extracted. The fit function used is²⁵

$$\frac{dP}{dH} = K_1 \frac{4\Delta H(H - H_{res})}{[4(H - H_{res})^2 + (\Delta H)^2]^2} - K_2 \frac{(\Delta H)^2 - 4(H - H_{res})^2}{[4(H - H_{res})^2 + (\Delta H)^2]^2} + K_3 H + K_4, \quad (1)$$

where K_1 , K_2 , K_3 , and K_4 represent the symmetric, antisymmetric, slope, and a constant factor, respectively.

In Fig. 1(d), the data are fitted to the Kittel equation

$$f = \gamma/2\pi \sqrt{H(H + M_{eff})}, \quad (2)$$

where γ is the gyromagnetic ratio and M_{eff} is the effective magnetization. Using the dispersion relation, we extract $\gamma/2\pi$ and M_{eff} at different temperatures. The line in Fig. 1(e) shows a linear fit to $\Delta H_{FMR} = \Delta H_0 + (2\alpha/\gamma)2\pi f$, where ΔH_0 describes the inhomogeneous broadening and α is the Gilbert damping. Note that the slope of the fitted lines is temperature dependent. This reflects the temperature dependence of the Gilbert damping, Fig. 2(c), since the gyromagnetic ratio is temperature independent, Fig. 2(a), as discussed below.

Figure 2 shows the variation of the gyromagnetic ratio, the effective magnetization, the Gilbert damping, and inhomogeneous broadening as a function of the temperature. Four points should be mentioned here regarding 2(a)–2(d): First, the $\gamma/2\pi$ has a constant value of 3 MHz/Oe and does not vary as the temperature changes. Its value is very near to the standard value of 2.8 MHz/Oe. Second, the effective magnetization increases as the temperature decreases. The $4\pi M_{eff}$ is equal to 2866 G at room temperature and 4300 G

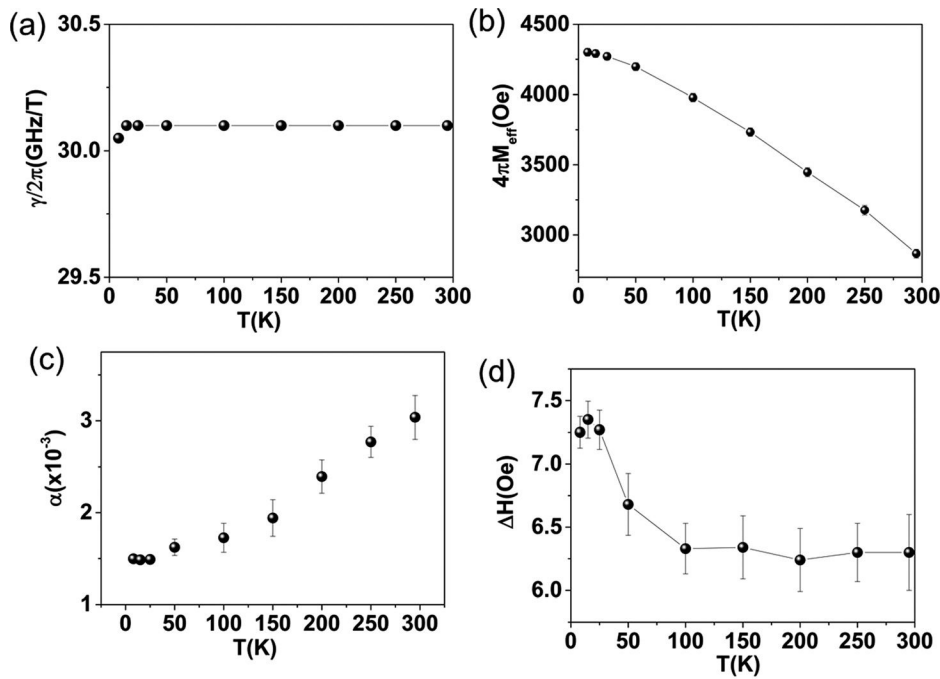


FIG. 2. Variation of the magnetodynamic parameters as a function of the temperature for the 30 nm thick film: (a) gyromagnetic ratio; (b) $4\pi M_{eff}$; (c) Gilbert damping; and (d) the inhomogeneous broadening.

at 8 K. The tabulated bulk value of the saturation magnetization for YIG is 1760 G at 295 K and 2470 G at 4 K. A similar increase in the PLD-grown YIG magnetization has been reported and attributed to strong uniaxial anisotropy caused by Fe^{3+} vacancies within octahedral sites.^{16,17} Third, the Gilbert damping increases as the temperature increases. In bulk YIG, the increase of the Gilbert damping with temperature was also reported.²⁷⁻²⁹ At room temperature, the damping value of the film is about 3.2×10^{-3} , and it drops to 1.6×10^{-3} at 8 K. The measured value of Gilbert damping is larger than that of the PLD films,^{15,17} but comparable to that of the sputtered films.¹⁹ Despite the large value of the damping coefficient, it has a clear temperature dependence, due to the relaxation of the magnetization with thermal scattering as magnons and phonons. Fourth, the inhomogeneous broadening, Fig. 2(d), increases slightly with the temperature and forms a peak around 20 K. It then decreases slowly at 8 K. The temperature dependence is only due to the film itself. Such an effect has been observed in bulk YIG doped with rare-earth metals.³⁰ Our YIG films may contain ions of rare-earth series due to the target impurities. Target component Y_2O_3 of 99.99% purity (standard for target) contains, for

example, Dy atoms at concentration of 5×10^{-5} .³¹ The spin-lattice relaxation rate in iron garnets containing ions of the rare-earth series even at less concentration features a peak at low temperature, as was estimated in Ref. 23.

The increase in the Gilbert damping versus the temperature was observed for films with different film thicknesses, as shown in Fig. 3(a). The Gilbert damping as a function of film thickness at $T = 295$ K (black symbols) and $T = 8$ K (red symbols) is shown in the inset of Fig. 3(a). It could be observed that the damping coefficient increases as the thickness decreases at $T = 295$ K. Such behavior has been reported previously.²⁶ The thickness dependence of the damping is attributed either to a compromised YIG-film quality for the thinnest YIG films or to magnon-magnon scattering process at the interface, which would be enhanced for thinner films and would give rise to an enhancement of the damping coefficient, compared to the thicker films. At low temperatures, the Gilbert damping for different film thicknesses, Fig. 3(a), converges to a similar value which, in addition to the size of the error bars, results in a high degree of overlap between the different film thicknesses. However, at $T = 8$ K, it can be seen that the damping coefficient is

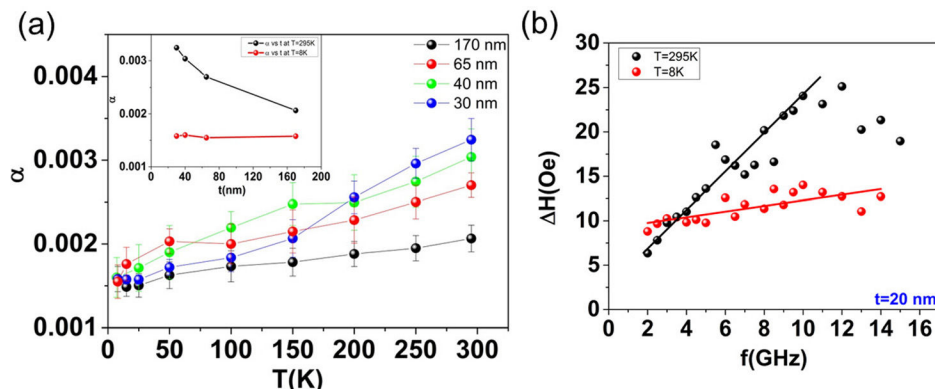


FIG. 3. (a) Variation of the Gilbert damping coefficient as a function of the temperature for different film thicknesses. (Inset) Variation of the damping as a function of the film thickness at $T = 295$ K (black) and $T = 8$ K (red). (b) The variation of the linewidth as a function of the frequency for a 20 nm thick film at $T = 295$ K (black) and $T = 8$ K (red).

independent of the thickness. The behavior of the damping as a function of the thickness at room temperature and low temperature has the following two characteristics: (1) as the YIG-film thickness decreases the surface-to-volume ratio increases, and the damping shows an expected increase at room temperature; (2) the relaxation process has an interesting temperature dependence where its effect on the damping is gradually reduced as the temperature decreases and becomes virtually absent at 8 K. We attribute this trend in the damping to the presence of defects and impurities at the surface, which are the most likely contributors to enhancing magnon–magnon scattering.³² To investigate this behavior further, we measured a 20 nm thin film grown using the same deposition conditions. We observed a nonlinear dependence of the linewidth on the frequency measured at room temperature (red circles), as shown in Fig. 3(b). The linewidth increases linearly until $f=9$ GHz, before forming a maximum and dropping down again at higher frequencies. This behavior is generally attributed to magnon–magnon scattering.^{17,24} For measurements of this film at the low temperature ($T=8$ K), the nonlinear dependence disappears, and the linewidth increases almost linearly with the frequency. This strongly validates the above explanation for the measured trend in the damping.

In summary, we performed FMR measurements on YIG thin films grown by PLD of varying thicknesses and as a function of temperature. First, a clear temperature dependence of the damping was observed. Second, the thickness variation of the damping changes with temperature, which was attributed to the scattering of magnons by defects and impurities on the surfaces.

This work was supported by the Swedish Foundation for Strategic Research (SSF), the Swedish Research Council (VR), and The Knut and Alice Wallenberg foundation (KAW). This work was also supported by the European Research Council (ERC) under the European Community's Seventh Framework Programme (FP/2007-2013)/ERC Grant 307144 "MUSTANG."

¹A. Khitun, M. Bao, and K. L. Wang, *J. Phys. D: Appl. Phys.* **43**, 264005 (2010).

²V. V. Kruglyak, S. O. Demokritov, and D. Grundler, *J. Phys. D: Appl. Phys.* **43**, 264001 (2010).

³J. E. Mee, J. L. Archer, R. H. Meade, and T. N. Hamilton, *Appl. Phys. Lett.* **10**, 289 (1967).

⁴A. A. Serga, A. V. Chumak, and B. Hillebrands, *J. Phys. D: Appl. Phys.* **43**, 264002 (2010).

⁵M. Sparks, *Ferromagnetic-Relaxation Theory* (McGraw-Hill, New York, 1964).

⁶Y. Kajiwara, K. Harii, S. Takahashi, J. Ohe, K. Uchida, M. Mizuguchi, H. Umezawa, H. Kawai, K. Ando, K. Takanashi, S. Maekawa, and E. Saitoh, *Nature* **464**, 262 (2010).

⁷Y. Sun, H. Chang, M. Kabatek, Y. Y. Song, Z. Wang, M. Jantz, W. Schneider, M. Wu, E. Montoya, B. Kardasz, B. Heinrich, S. G. E. te Velthuis, H. Schultheiss, and A. Hoffmann, *Phys. Rev. Lett.* **111**, 106601 (2013).

⁸C. Hahn, G. de Loubens, O. Klein, M. Viret, V. V. Naletov, and J. Ben Youssef, *Phys. Rev. B* **87**, 174417 (2013).

⁹B. Heinrich, C. Burrowes, E. Montoya, B. Kardasz, E. Girt, Y.-Y. Song, Y. Sun, and M. Wu, *Phys. Rev. Lett.* **107**, 066604 (2011).

¹⁰A. V. Chumak, A. A. Serga, M. B. Jungfleisch, R. Neb, D. A. Bozhko, V. S. Tiberkevich, and B. Hillebrands, *Appl. Phys. Lett.* **100**, 082405 (2012).

¹¹V. Castel, N. Vlietstra, J. B. Youssef, and B. J. van Wees, *Appl. Phys. Lett.* **101**, 132414 (2012).

¹²M. B. Jungfleisch, V. Lauer, R. Neb, A. V. Chumak, and B. Hillebrands, *Appl. Phys. Lett.* **103**, 022411 (2013).

¹³O. Mosendz, J. E. Pearson, F. Y. Fradin, G. E. W. Bauer, S. D. Bader, and A. Hoffmann, *Phys. Rev. Lett.* **104**, 046601 (2010).

¹⁴K.-I. Uchida, H. Adachi, T. Ota, H. Nakayama, S. Maekawa, and E. Saitoh, *Appl. Phys. Lett.* **97**, 172505 (2010).

¹⁵Y. Y. Sun, Y. Y. Song, H. C. Chang, M. Kabatek, M. Jantz, W. Schneider, M. Z. Wu, H. Schultheiss, and A. Hoffmann, *Appl. Phys. Lett.* **101**, 152405 (2012).

¹⁶S. A. Manuilov, S. I. Khartsev, and A. M. Grishin, *J. Appl. Phys.* **106**, 123917 (2009).

¹⁷O. d'Allivy Kelly, A. Anane, R. Bernard, J. B. Youssef, C. Hahn, A. H. Molpeceres, C. Carretero, E. Jacquet, C. Deranlot, P. Bortolotti, R. Lebourgeois, J.-C. Mage, G. de Loubens, O. Klein, V. Cros, and A. Fert, *Appl. Phys. Lett.* **103**, 082408 (2013).

¹⁸C. Hahn, V. V. Naletov, G. de Loubens, O. Klein, O. d'Allivy Kelly, A. Anane, R. Bernard, E. Jacquet, P. Bortolotti, V. Cros, J. L. Prieto, and M. Munoz, *Appl. Phys. Lett.* **104**, 152410 (2014).

¹⁹T. Liu, H. Chang, V. Vlaminck, Y. Sun, M. Kabatek, A. Hoffmann, L. Deng, and M. Wu, *J. Appl. Phys.* **115**, 17A501 (2014).

²⁰N. Vlietstra, J. Shan, V. Castel, B. J. van Wees, and J. B. Youssef, *Phys. Rev. B* **87**, 184421 (2013).

²¹H. Nakayama, M. Althammer, Y.-T. Chen, K. Uchida, Y. Kajiwara, D. Kikuchi, T. Ohtani, S. Geprägs, M. Opel, S. Takahashi, R. Gross, G. E. W. Bauer, S. T. B. Goennenwein, and E. Saitoh, *Phys. Rev. Lett.* **110**, 206601 (2013).

²²S. R. Marmion, M. Ali, M. McLaren, D. A. Williams, and B. J. Hickey, *Phys. Rev. B* **89**, 220404(R) (2014).

²³G. F. Dionne and G. L. Fitch, *J. Appl. Phys.* **87**, 4963 (2000).

²⁴R. Arias and D. L. Mills, *Phys. Rev. B* **60**, 7395 (1999).

²⁵G. Woltersdorf, "Spin pumping and two-magnon scattering in magnetic multilayers," Ph.D. thesis, Simon Fraser University, 2004.

²⁶M. B. Jungfleisch, A. V. Chumak, A. Kehlberger, V. Lauer, D. H. Kim, M. C. Onbasli, C. A. Ross, M. Kläui, and B. Hillebrands, e-print [arXiv:1308.3787](https://arxiv.org/abs/1308.3787).

²⁷M. Sparks and C. Kittel, *Phys. Rev. Lett.* **4**, 232 (1960).

²⁸E. G. Spencer and R. C. LeCraw, *Phys. Rev. Lett.* **4**, 130 (1960).

²⁹E. G. Spencer, R. C. LeCraw, and R. C. Linarks, *Phys. Rev.* **123**, 1937 (1961).

³⁰P. E. Seiden, *Phys. Rev.* **133**, A728 (1964).

³¹G. Winkler and P. Hansen, *Mater. Res. Bull.* **4**, 825 (1969).

³²The magnon-phonon interaction may also contribute to the measured damping in the films even at $T=8$ K where this interaction is very weak. However, this interaction will contribute to the bulk part of the damping and hence it will not depend on the film thickness.